Chemical Physics 70 (1982) 139–147
North-Holland Publishing Company

ELECTRONIC EXCITED STATE TRANSPORT AND TRAPPING IN ONE- AND TWO-DIMENSIONAL DISORDERED SYSTEMS

Roger F. LORING and M.D. FAYER
Department of Chemistry, Stanford University, Stanford, CA 94305, USA

Received 7 December 1981

A theoretical study of incoherent transport and trapping of electronic excitations in disordered one- and two-dimensional systems is carried out. These systems contain randomly distributed donor and trap species. Transport is described by a master equation. The diagrammatic expansion of the Green function developed by Gochanour, Andersen and Fayer is applied to this problem, and experimentally observable transport properties are calculated. The calculation of the relative integrated trap emission is described, and the effect on this observable of changing the distance dependence of the intermolecular transfer rate is discussed. The model is shown to accurately describe the results of experiments by Kopelman and coworkers on singlet energy transport in mixed naphthalene crystals.

1. Introduction

In a recent paper, hereafter referred to as I, Loring et al. [1] presented a theory of the transport and trapping of electronic excitations in a two-component disordered system. Paper I is an extension of the work of Gochanour, Andersen, and Fayer (hereafter referred to as GAF) who treated electronic excited state energy transport in a one-component system of randomly distributed particles [2]. In the GAF theory, transport is incoherent and is described by a master equation. A diagrammatic technique is used to obtain a hierarchy of self-consistent approximations to the system's Green function, from which transport properties such as the time-dependent generalized diffusion coefficient can be calculated. The GAF formalism, and its extensions to include trapping are applicable to any dimensionality and intermolecular transfer rate. Specific results for the three-dimensional trapping problem with species interacting via a Förster dipole–dipole interaction [3] were presented in I.

In many molecular crystals, the excitation transfer interactions are highly anisotropic and energy transport is approximately one or two dimensional. Systems in which the intermolecular interactions are close to one dimensional include 1,4-dibromonaphthalene [4] and tetrachlorobenzene [5]. Kopelman and coworkers have carried out extensive investigations of both singlet [6–8] and triplet [6,9] excited state energy transport and trapping in mixed naphthalene crystals, an approximately two-dimensional energy transport system [6,7,10]. Triplet energy transport and trapping in another two-dimensional system, pyrazine, have been studied by Zewail and co-workers [11].

In the present work, we apply the formalism of I to one- and two-dimensional systems of static, randomly distributed donor and trap species. Excitations are transported from donor to donor and donor to trap, but detrapping is excluded. In section 2, we briefly review the modifications of the GAF theory presented in I. Section 3 contains the applications of this theory to one- and two-dimensional systems. We also show that within our self-consistent approximation transport becomes diffusive in the long-time limit for one- component, one- and two-dimensional random systems with a dipolar transfer rate. In section 4, we compare our theoretical results to data from the steady-state experiments of Kopelman et al. [6–10] on mixed naphthalene crystals, and consider the question of percolation. It is found that the master equation approach presented here can accurately describe the naphthalene singlet data, provided an octupole–octupole interaction is used. Furthermore, if an intermolecular interaction which terminates abruptly with distance is used, as is

0301-0104/82/0000–0000/$ 02.75 © 1982 North-Holland

necessary to be consistent conceptually with the original formulation of the site percolation problem [12], the data cannot be reproduced. Section 5 contains our conclusions.

2. The master equation and Green function

The system consists of N donor molecules and M trap molecules randomly distributed in a volume Ω, with number densities ρ_D and ρ_T, respectively. The donor molecules are labeled 1 through N, and the trap molecules $N+1$ through $N+M$. The probability that an excitation is on the jth molecule in configuration $R = (r_1, r_2 \ldots r_{N+M})$ at time t, $p_j'(R, t)$, satisfies the master equation [1,2]

$$\frac{\mathrm{d}p_j'}{\mathrm{d}t} = \sum_{k=1}^{N} w_{jk}(p_k' - p_j') - \sum_{k=N+1}^{N+M} v_{kj}p_j' - p_j'/\tau_D, \quad j \leqslant N,$$

$$\frac{\mathrm{d}p_j'}{\mathrm{d}t} = \sum_{k=1}^{N} v_{jk}p_k' - p_j'/\tau_T, \quad N+1 \leqslant j \leqslant N+M. \qquad (1)$$

The distance-dependent transfer rates between two donor molecules and a donor molecule and a trap molecule are given by $w_{jk}(r_{jk})$ and $v_{jl}(r_{jl})$. The transfer rates are taken to be independent of orientation and only dependent on distance. For a random system, the use of an orientation-dependent transfer rate will not change the form of the results, but will make small numerical differences [13]. w_{jj} is defined to be zero. The donor–donor transfer rate is assumed to be symmetric: $w_{jk} = w_{kj}$. τ_D and τ_T are the measured lifetimes of the excitation on the donor and the trap, respectively, in the absence of intermolecular energy transfer. For convenience, we first consider a system in which the excitations are infinitely long lived. From these results, the transport properties of a system in which the excitation has finite lifetimes on the donor and trap species may be easily calculated.

Our goal is the calculation of the Green function, from which the system's transport properties can be calculated. The Green function $G(r, r', t)$ gives the conditional probability of finding an excitation at position r and time t, given that it was at position r' at $t = 0$. $G(r, r', t)$ can be written as the sum of three terms [1,2]:

$$G(r, r', t) = G^S(r-r', t) + G^m(r-r', t) + G^T(r-r', t). \qquad (2)$$

The integral of $G^S(r-r', t)$ over a small volume about r' gives the probability that the excitation is on the initially excited site at time t. $G^m(r-r', t)$ and $G^T(r-r', t)$ are measures of the probability of finding the excitation on a donor site other than the initial one, and on a trap site, respectively.

It is most convenient to work with the Laplace–Fourier transform of the Green function, given by

$$\hat{G}(k, \epsilon) = \int_0^\infty \mathrm{e}^{-\epsilon t} \int \mathrm{d}r\, \mathrm{e}^{\mathrm{i}k\cdot r}\, G(r, t). \qquad (3)$$

Transforming the formal solution for the Green function gives [1,2]

$$\hat{G}^S(\epsilon) = \langle [(\epsilon I - Q)^{-1}]_{11} \rangle, \qquad (4)$$

$$\hat{G}^m(k, \epsilon) = (N-1)\langle \exp(\mathrm{i}k\cdot r_{12})[(\epsilon I - Q)^{-1}]_{21} \rangle, \qquad (5)$$

$$\hat{G}^T(k, \epsilon) = M\langle \exp(\mathrm{i}k\cdot r_{1,N+1})[(\epsilon I - Q)^{-1}]_{N+1,1} \rangle, \qquad (6)$$

where I is the unit matrix, and the brackets denote a configuration average over the positions of all donors and traps.

The matrix Q is defined by

$$Q_{jk} = w_{jk} - \delta_{jk}\left(\sum_{l=1}^{N} w_{lk} + \sum_{i=N+1}^{N+M} v_{ik}\right), \quad j, k \leqslant N,$$

$$Q_{jk} = v_{jk}, \quad N+1 \leqslant j \leqslant N+M, \quad k \leqslant N,$$

$$Q_{jk} = 0, \quad k > N. \qquad (7)$$

When the matrix $(\epsilon I - Q)^{-1}$ is expanded in powers of ϵ and Q, Eqs. (4)–(6) become infinite series of integrals of products of w_{ij} and v_{ij} transfer rates. Each integral can be represented with a diagram [2]. The self-consistent approximation to the Green function is carried out as follows [1,2]. The $\hat{G}^m(k, \epsilon)$ diagrammatic series can be rewritten in terms of a subset of $\hat{G}^m(k, \epsilon)$ diagrams from which all other $\hat{G}^m(k, \epsilon)$ diagrams can be generated. This simpler series, $\tilde{\Delta}(k, \hat{G}^S(\epsilon))$, is a function of $\hat{G}^S(\epsilon)$. Similarly, the diagrammatic series for $\hat{G}^T(k, \epsilon)$ may be generated from a simpler series, $\tilde{\Gamma}(k, \epsilon, \hat{G}^S(\epsilon))$, also a function of $\hat{G}^S(\epsilon)$. The relationship between $\tilde{\Gamma}(k, \epsilon, \hat{G}^S(\epsilon))$ and $\hat{G}^T(k, \epsilon)$, and

$\tilde{\Delta}(k, \hat{G}^s(\epsilon))$ and $\hat{G}^m(k, \epsilon)$ together with the fact that the integral of the complete Green function over the system volume must be unity gives rise to a self-consistent equation for $\hat{G}^s(\epsilon)$. Our approach is to approximate the diagrammatic series for $\tilde{\Delta}(k, \hat{G}^s(\epsilon))$ and $\tilde{\Gamma}(k, \epsilon, \hat{G}^s(\epsilon))$ in terms of $\hat{G}^s(\epsilon)$, solve for $\hat{G}^s(\epsilon)$ self-consistently, and then use this value of $\hat{G}^s(\epsilon)$ in our approximate $\tilde{\Delta}(k, \hat{G}^s(\epsilon))$ and $\tilde{\Gamma}(k, \epsilon, \hat{G}^s(\epsilon))$ to generate $\hat{G}^m(k, \epsilon)$ and $\hat{G}^T(k, \epsilon)$. In this work we will use the "two-body" approximation to $\tilde{\Delta}(k, \epsilon, \hat{G}^s(\epsilon))$ and $\tilde{\Gamma}(k, \epsilon, \hat{G}^s(\epsilon))$ described in I. It must be emphasized that the "two-body" approximation is not the first term in a density expansion, but rather an approximation containing an infinite number of high-order diagrams. From our previous work, we expect the two-body results to be physically realistic for all times and concentrations, but to be most accurate at short times and low concentrations. The self-consistent equation for $\hat{G}^s(\epsilon)$ is [1,2]

$$[\hat{G}^s(\epsilon)]^2 + [\tilde{\Gamma}(0, \epsilon, \hat{G}^s(\epsilon)) - 1/\epsilon]\,\hat{G}^s(\epsilon) + \tilde{\Delta}(0, \hat{G}^s(\epsilon))/\epsilon = 0. \quad (8)$$

The two-body approximations to $\tilde{\Delta}(k, \hat{G}^s(\epsilon))$ and $\tilde{\Gamma}(k, \epsilon, \hat{G}^s(\epsilon))$ are given by

$$\tilde{\Delta}(k, \hat{G}^s(\epsilon)) = \rho_D [\hat{G}^s(\epsilon)]^2 \times \int d\boldsymbol{r} \exp(i\boldsymbol{k}\cdot\boldsymbol{r}) \frac{w(r)}{1 + 2\hat{G}^s(\epsilon)\, w(r)}, \quad (9)$$

$$\tilde{\Gamma}(k, \epsilon, \hat{G}^s(\epsilon)) = (\rho_T/\epsilon)[\hat{G}^s(\epsilon)] \times \int d\boldsymbol{r} \exp(i\boldsymbol{k}\cdot\boldsymbol{r}) \frac{v(r)}{1 + \hat{G}^s(\epsilon)\, v(r)}, \quad (10)$$

where $w(r)$ and $v(r)$ are the donor–donor and donor–trap transfer rates and ρ_D and ρ_T are the donor and trap number densities [1,2].

The probability that an excitation is on a donor at a given time after the system has been excited can be measured directly in time-resolved studies of energy transport. We define $G^D(r, t)$ as the probability that an excitation is on some donor site at position r and time t. Since the excitation may be either on the initially excited donor site or on another donor site, $G^D(r, t)$ must be the sum of $G^s(t)$ and $G^m(r, t)$. The $k = 0$ limit of the Laplace–Fourier transform of $G^D(r, t)$ is given by

$$\hat{G}^D(0, \epsilon) = [\hat{G}^s(\epsilon)]^2/[\hat{G}^s(\epsilon) - \tilde{\Delta}(0, \hat{G}^s(\epsilon))]. \quad (11)$$

The inverse transform of this function gives the probability that an excitation is somewhere in the donor ensemble. For a real system, in which the excitation has a finite lifetime on the donor species, the inverse transform of eq. (11) should be multiplied by a decaying exponential. The Laplace transform of the probability that an excitation is on a trap, for a system with finite donor and trap lifetimes, was also given in I:

$$\hat{N}^T(\epsilon) = [1 - (\epsilon + k_D)\,\hat{G}^D(0, \epsilon + k_D)]/(\epsilon + k_T), \quad (12)$$

where k_D and k_T are the inverses of the donor and trap lifetimes, respectively.

3. Transport properties of one- and two-dimensional random systems

Consider a one-dimensional system of randomly distributed donors and traps having multipolar excitation transfer rates. The donor–donor excitation transfer rate $w(r)$ and the donor–trap excitation transfer rate $v(r)$ are given by:

$$w(r) = (R^{DD}/r)^n/\tau_D,$$

$$v(r) = (R^{DT}/r)^m/\tau_D, \quad (13)$$

where τ_D is the measured lifetime of the excitation on the donor in the absence of energy transport. The strengths of the donor–donor and donor–trap interactions are characterized by R^{DD} and R^{DT}, respectively. $R^{DD}(R^{DT})$ is the interparticle separation at which the rate of excitation transfer from an excited donor to a donor (trap) equals the rate of all other excited state decay processes. Substituting eq. (13) into eqs. (9) and (10) gives

$$\tilde{\Delta}(0, \hat{G}^s(\epsilon)) = (C_D/\tau_D^{1/n})\,[(\pi/n)\csc(\pi/n)] \times [\hat{G}^s(\epsilon)]^{1+1/n} 2^{1/n-1}, \quad (14)$$

$$\tilde{\Gamma}(0, \epsilon, \hat{G}^s(\epsilon)) = (C_T/\tau_D^{1/m})\,[(\pi/m)\csc(\pi/m)] \times [\hat{G}^s(\epsilon)]^{1/m}/\epsilon, \quad (15)$$

where C_D and C_T are reduced donor and trap concentrations given by

$$C_D = 2R^{DD}\rho_D, \qquad C_T = 2R^{DT}\rho_T. \tag{16}$$

For dipole–dipole transfer $m = n = 6$, and the R parameters in eq. (13) become R_0^{DD} and R_0^{DT}, in accordance with the notation of Förster [3]. For this case, the self-consistent equation, eq. (8), is a sixth-order algebraic equation in $[\hat{G}^s(\epsilon)]^{1/6}$:

$$\hat{G}^s(\epsilon) + (\pi/3\epsilon\tau_D^{1/6})(C_T + 2^{-5/6}C_D) \times [\hat{G}^s(\epsilon)]^{1/6} - 1/\epsilon = 0. \tag{17}$$

This equation has two real roots, only one of which results in a decreasing function of time, which is necessary to be consistent with the definition of $\hat{G}^s(\epsilon)$. If this result for $\hat{G}^s(\epsilon)$ is substituted into eqs. (14), (11), and (12), the donor and trap excitation dynamics can be calculated.

The generalized diffusion coefficient, $D(r, t)$ and mean squared displacement of the excitation, $\langle r^2(t)\rangle$ can be calculated from the Green function as described by GAF. The Laplace transform of the mean squared displacement is related to the $k = 0$ Laplace–Fourier transform of the diffusion coefficient by

$$\langle r^2(\epsilon)\rangle = (l/\epsilon^2)\hat{D}(0, \epsilon), \tag{18}$$

where l equals 6, 4, or 2 for transport in 3, 2, or 1 dimensions. If transport were diffusive at all times, $\hat{D}(0, \epsilon)$ would not be a function of ϵ. For transport to become diffusive in the long-time limit, the following limit must exist:

$$\lim_{\epsilon \to 0} \hat{D}(0, \epsilon) = \hat{D}(0, 0). \tag{19}$$

Gochanour et al. [2] showed that this limit exists in their self-consistent approximation for a one-component random system in three dimensions with dipole–dipole interactions. It was shown in I that the limit in eq. (19) is zero for a system with traps, since at long times all excitations will be trapped. Förster [3] showed that dipole–dipole energy transfer on a three-dimensional one-component lattice is diffusive, and calculated diffusion constants for several lattice types. The two-body diffusion constant calculated by GAF for the random system has the same functional form as Förster's result with a numerical coefficient that is 18% larger than the result for a cubic lattice.

We find that for a one-component system ($C_T = 0$) of randomly distributed particles in one dimension with dipole–dipole interactions, the limit in eq. (19) exists. Transport is in general not diffusive, but a diffusion constant exists in the long-time limit:

$$\hat{D}(0, \epsilon) = 0.185\, C_D (R_0^{DD})^2\, [\tau_D \hat{G}^s(\epsilon)]^{-1/2}, \tag{20}$$

$$\lim_{\epsilon \to 0} \hat{D}(0, \epsilon) = \hat{D}(0, 0) = 0.0376\, C_D^4 (R_0^{DD})^2/\tau_D. \tag{21}$$

We also carried out a calculation analogous to that of Förster for a one-dimensional "lattice" of evenly spaced sites. The result is

$$D = 0.0676\, C_D^4 (R_0^{DD})^2/\tau_D. \tag{22}$$

Again, the concentration dependence is the same for the random system and the lattice, but unlike the three-dimensional case, transport for a given reduced concentration is more rapid on the lattice than in the random system. In a random system, transport will be slowed when an excitation reaches a region of low local density. One would expect this effect to be much more pronounced in one dimension, where an excited particle has only two near neigbors, than in two or three dimensions.

We now consider a two-dimensional system of randomly distributed donors and traps, interacting with a multipolar transfer rate [eq. (13)]. Eqs. (9) and (10) give

$$\tilde{\Delta}(0, \hat{G}^s(\epsilon)) = 2^{2/n}\,(\pi/n)\,\csc(2\pi/n)\,\tau_D^{-2/n} \times C_D [\hat{G}^s(\epsilon)]^{1+2/n}, \tag{23}$$

$$\tilde{\Gamma}(0, \epsilon, \hat{G}^s(\epsilon)) = (2\pi/m)\,\csc(2\pi/m)\,\tau_D^{-2/m} \times C_T \epsilon^{-1} [\hat{G}^s(\epsilon)]^{2/m}, \tag{24}$$

where C_D and C_T are reduced concentrations defined by

$$C_D = \pi(R^{DD})^2\rho_D, \qquad C_T = \pi(R^{DT})^2\rho_T. \tag{25}$$

For dipole–dipole transfer, the self-consistent equation, eq. (8), is now cubic in $[\hat{G}^s(\epsilon)]^{1/3}$ with one real root:

$$\hat{G}^s(\epsilon) + (2^{1/3}\pi/3^{3/2}\tau_D^{1/3}\epsilon)\,(C_D + 2^{2/3}C_T) \times [\hat{G}^s(\epsilon)]^{1/3} - 1/\epsilon = 0. \tag{26}$$

From the solution to eq. (26), the system's transport properties can be calculated in the two-body approximation as discussed above.

By setting C_T to zero in eq. (26), we can calculate properties of a one-component system. We find that transport becomes diffusive at long times for the one-component, two-dimensional random system with dipole interactions:

$$\hat{D}(0,\epsilon) = [\pi C_D (R_0^{DD})^2/\tau_D^{2/3} 2^{4/3} 3^{3/2}]\,[\hat{G}^S(\epsilon)]^{-1/3}, \quad (27)$$

$$\lim_{\epsilon \to 0} \hat{D}(0,\epsilon) = \hat{D}(0,0) = 0.183\,(R_0^{DD})^2 C_D^2/\tau_D. \quad (28)$$

A diffusion constant calculation for a two-dimensional square lattice and a dipole–dipole interaction using Förster's approach yields

$$D = 0.153\,(R_0^{DD})^2 C_D^2/\tau_D. \quad (29)$$

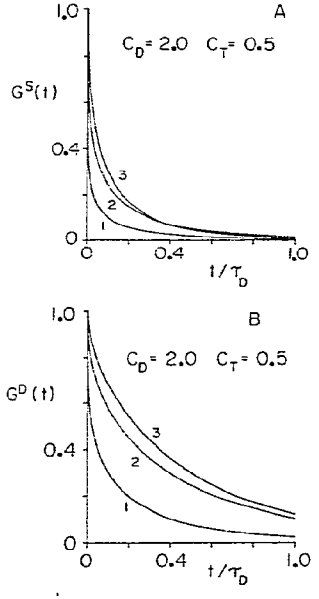

Fig. 1. (A) The time-dependent probability that an excitation is on the initial site in the two-body approximation for dipole–dipole transfer in one dimension (curve 1), two dimensions (curve 2), and three dimensions (curve 3). Reduced concentrations are $C_D = 2.0$, $C_T = 0.5$. Lifetime decay not included. (B) The time-dependent probability that an excitation is in the donor ensemble in the two-body approximation for dipole–dipole transfer in one dimension (curve 1), two dimensions (curve 2), and three dimensions (curve 3). $G^D(t)$ is the inverse Laplace transform of $\hat{G}^D(0,\epsilon)$, defined in eq. (11). Lifetime decay not included. Reduced concentrations are the same as in A.

As in the three-dimensional case discussed by GAF, the concentration dependence of the lattice diffusion constant is the same as for $\hat{D}(0,0)$, with $\hat{D}(0,0)$ having a slightly larger numerical coefficient.

In fig. 1A, we show the function $G^S(t)$, the probability that an excitation is on the initial site in the two-body approximation for Förster dipole–dipole transfer. Curves 1, 2, and 3 are $G^S(t)$ for one, two, and three dimensions, respectively, for $C_D = 2.0$ and $C_T = 0.5$. The reduced concentration C_D (C_T) gives the average number of donors (traps) within a distance R_0^{DD} (R_0^{DT}) of a given donor. $G^D(t)$, the probability that an excitation has not been trapped, is shown in fig. 1B for the same reduced concentrations. Again curves 1, 2, and 3 are for one, two, and three dimensions. For a given pair of reduced concentrations, trapping is much faster in one dimension that in two or three. Inverse Laplace transforms for fig. 1 were carried out numerically using the Stehfest method [14].

4. Application to steady-state experiments: exciton percolation

Singlet and triplet energy transport and trapping in an effectively two-dimensional system (perdeuteronaphthalene/naphthalene/betamethylnaphthalene (BMN) mixed crystals) have been extensively studied by Kopelman and co-workers [6–10]. In these steady-state experiments, the integrated emission from the naphthalene donors and the BMN traps is measured at fixed, very low trap concentrations for a series of donor concentrations. The results are best illustrated by plots of integrated trap emission normalized by the total integrated emission (trap + donor) versus donor concentration. These plots show that transport to the traps increases very slowly with increasing donor concentration until a critical donor concentration is reached at which trapping becomes very efficient, and a substantial fraction of the total emission comes from the traps. As the donor concentration is further increased, the relative emission from the trap rises rapidly to unity.

This behavior is easily interpreted for a system with low enough trap concentration that most trapping events must result from a series of donor–donor transfers leading to the final donor–trap transfer. At low donor concentrations, most excitations will be restricted to single donors or small clusters of donors. Since

the trap concentration is low, little trapping will occur. As the donor concentration is raised, a point will be reached where paths of interacting donors leading to all traps will be formed, and most of the excitations will be trapped.

The relative integrated trap emission, $I(C_D, C_T)$, can be calculated from the master equation Green function discussed in section 2. $G^D(t)$, the inverse Laplace transform of $\hat{G}^D(0, \epsilon)$ [eq. (11)], when multiplied by $\exp(-k_D t)$, gives the probability that an excitation with donor lifetime k_D^{-1} is on a donor. The inverse Laplace transform of eq. (12) gives $N^T(t)$, the probability that an excitation with lifetimes k_D^{-1} and k_T^{-1} for donors and traps, respectively, is on a trap. $I(C_D, C_T)$ is given by

$$I(C_D, C_T) = \frac{k_T q_T \int_0^\infty N^T(t)\,dt}{k_T q_T \int_0^\infty N^T(t)\,dt + k_D q_D \int_0^\infty G^D(t) e^{-k_D t}\,dt} \tag{30}$$

$$= \frac{k_T q_T \hat{N}^T(\epsilon = 0)}{k_T q_T \hat{N}^T(\epsilon = 0) + k_D q_D \hat{G}^D(0, \epsilon = k_D)}. \tag{31}$$

q_T and q_D are the trap and donor quantum yields (ratio of measured lifetime to radiative lifetime), respectively, in the absence of energy transport. Substituting eqs. (11) and (12) into eq. (31) yields

$$I(C_D, C_T) = \frac{1 - k_D \hat{G}^D(0, \epsilon = k_D)}{1 + k_D \hat{G}^D(0, \epsilon = k_D)(q_D/q_T - 1)}. \tag{32}$$

We consider the experimentally studied [6–10,15] limit ($C_T \to 0$) of eq. (32) for a two-dimensional disordered system with multipolar excitation transfer rates as in eq. (13). If $m = n$ in eq. (13), the self-consistent equation for $\hat{G}^s(\epsilon)$, eq. (8), in the two-body approximation is an algebraic equation of order $m/2$. $I(C_D, C_T)$ is calculated by solving this equation numerically at $\epsilon = k_D$ and using eqs. (11), (23) and (32). In the $C_T \to 0$ limit, plots of $I(C_D, C_T)$ versus C_D for different C_T and different values of q_D/q_T can be represented by a single plot of $I(\tilde{C})$, where $\tilde{C}$ is the reduced donor concentration, eq. (25), scaled by an arbitrary criterion. We shall take $\tilde{C}$ to be the reduced donor concentration divided by the value of C_D for which $I(C_D, C_T) = 0.5$. In the $C_T \to 0$ limit, changing C_T does not change the shape of the curve, but merely scales the C_D axis. We find that for a dipole–dipole transfer rate, $I(\tilde{C})$ rises smoothly from zero to unity without displaying the sudden onset of trapping which is characteristic of the naphthalene data. As the exponent in the transfer rate is raised from 6, $I(\tilde{C})$ begins to display the sharp inflection point shown by the data. The higher the exponent, the steeper the curve becomes. Plots for $1/r^6$, $1/r^{10}$, and $1/r^{18}$ transfer rates are shown in fig. 2. The $1/r^{14}$ results were found to give the best fit to the singlet naphthalene data [7], as shown in fig. 3. The data were fit by assuming $q_D = q_T$ and $R^{DD} = R^{DT} = R$ in eq. (32). Since the quantity $k_D \hat{G}^D(0, \epsilon = k_D)$ is independent of k_D, R is the only adjustable parameter. The BMN mole fraction in these experiments was $\approx 10^{-3}$ [7]. If a BMN mole fraction of 1×10^{-3} is assumed, the resulting best value for R is ≈ 8 Å.

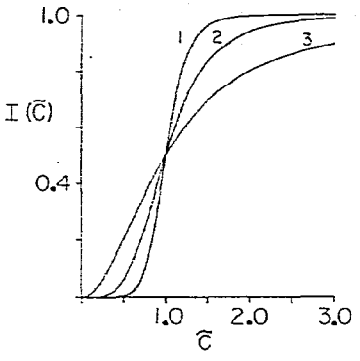

Fig. 2. The ratio of integrated trap emission to total integrated emission for a two-dimensional disordered system with a $1/r^{18}$ transfer rate (curve 1), a $1/r^{10}$ transfer rate (curve 2), and a $1/r^6$ transfer rate (curve 3). These results are in the $C_T \to 0$ limit. $\tilde{C}$ is the reduced donor concentration scaled by the concentration at which the ratio equals 0.5.

Within the framework of our model, the existence of a critical donor concentration at which trapping suddenly becomes efficient depends on the range of the transfer rate. The longer-ranged Förster transfer rate does not display this behavior, whereas the $1/r^{14}$ rate does. If transport is governed by a long-ranged interaction, significant trapping can occur at relatively low donor concentration.

To further investigate the effect of the range of the transfer rate on the integrated trap emission, we have

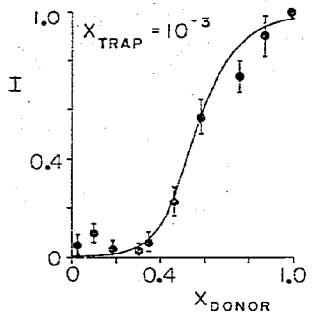

Fig. 3. The ratio of integrated trap emission to total integrated emission for singlet naphthalene, redrawn from ref. [7] X_{donor} is the mole fraction of naphthalene and X_{trap} is the mole fraction of betamethylnaphthalene (BMN) in a perdeuteronaphthalene/naphthalene/BMN mixed crystal. The solid line is our theoretical $I(C_D, C_T)$ [eq. (32)] for a $1/r^{14}$ transfer rate. See text.

considered the case in which the donor–donor transfer rate $w(r)$ and the donor–trap transfer rate $v(r)$ are of the following form:

$$w(r) = S, \quad r \leqslant d,$$
$$= 0, \quad r > d;$$
$$v(r) = S, \quad r \leqslant d,$$
$$= 0, \quad r > d. \qquad (33)$$

These transfer rates are parametrized by two quantities: d, a maximum interparticle separation for which the rate is finite, and S, the magnitude of the rate relative to the donor lifetime. This type of transfer rate is conceptually consistent with the original formulation of the site percolation problem [12], in which parts of a lattice are either connected or not connected, and in which there is nothing corresponding to the infinite range tail of a multipolar transfer rate.

The relation of the static site percolation problem to energy transfer dynamics of species distributed randomly on a lattice has been discussed in detail by Keyes and Pratt [16]. They argue that the solution of the master equation [our equation (1)] for an infinitely long-lived excitation and donor–donor and donor–trap transfer rates of finite range can be transformed into the solution of the percolation problem. Keyes and Pratt solve the master equation numerically for a finite two-dimensional square lattice. Their procedure is to generate random configurations of donors, all corresponding to a fixed donor concentration, on a finite lattice with a trap at the center, solve the master equation numerically for each configuration, and average the results. The relevant quantity is the probability that the trap is excited at infinite time. Their results for an infinitely long-lived excitation on a 9 X 9 lattice and transfer rates which are non-zero only for species occupying adjacent sites are reproduced in fig. 4A (dashed curve). In our notation this quantity is $\lim_{t\to\infty} G^T(t)$. For transfer rates of infinite range,

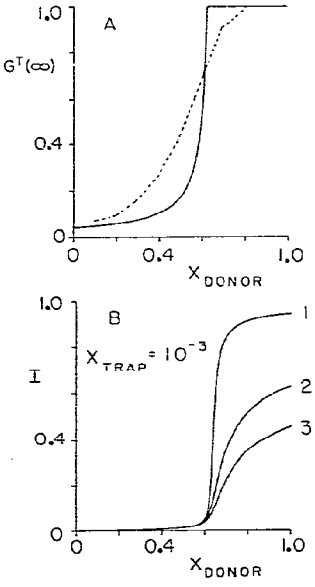

Fig. 4. (A) Probability that a trap is excited at infinite time for an excitation with infinite lifetimes on trap and donor. Dashed curve is reproduced from ref. [16] for a 9 X 9 square lattice with a trap at the center and nearest neighbor interactions only. Solid curve is our two-body result for an infinite two-dimensional random system with the transfer rates of eq. (33) for the corresponding donor and trap concentrations. The transfer rate range d in eq. (33) is equated to the lattice spacing. (B) The ratio of integrated trap emission to total integrated emission, $I(C_D, C_T)$, for an infinite two-dimensional random system with the transfer rates of eq. (33) is plotted versus donor concentration for fixed trap concentration. The trap concentration and donor concentration range correspond to those of the singlet naphthalene data (ref. [7]) shown in fig. 3. The maximum donor concentration equals that of a filled lattice of lattice spacing d, where d is the transfer rate range defined in eq. (33). The transfer rate magnitude S (hops/lifetime) is varied from 500 (curve 3) to 10^3 (curve 2) to 10^4 (curve 1).

such as the multipolar rates discussed above, $G^T(\infty)$ is always unity for an excitation with infinite lifetime, since an excited donor is never completely isolated with respect to energy transfer from all other donors and traps. However, with a transfer rate of finite range such as eq. (33), $G^T(\infty)$ will be less then unity for low donor concentrations at which some parts of the system can be isolated from the rest. For this case, $G^T(\infty)$ is determined by the "connectedness" of the system. Also shown in fig. 4A (solid curve) is $G^T(\infty)$ calculated with the self-consistent two-body approximation using the transfer rates of eq. (33), for an infinite two-dimensional system of randomly distributed donors and traps at concentrations corresponding to those of the Keyes and Pratt calculation. The plots for the finite lattice and the infinite random system both show an inflection point at donor concentrations near 0.59, the threshold percolation concentration for an infinite square lattice with nearest-neighbor interactions [16].

Using eq. (32), the relative integrated trap emission, $I(C_D, C_T)$, can be calculated for the case of an excitation with finite lifetime and the transfer rates of eq. (33). The parameter S (hops/lifetime) does not enter into the calculation of $G^T(\infty)$ described above, since the excitation was taken to be infinitely long lived. The calculation of $I(C_D, C_T)$ requires specifying S. Fig. 4B shows $I(C_D, C_T)$ for the transfer rate of eq. (33) at concentrations corresponding to those of the naphthalene data in fig. 3 [7]. For low values of S, $I(C_D, C_T)$ is less than unity at a donor concentration corresponding to a fully occupied lattice. As S is increased, the value of $I(C_D, C_T)$ at this maximum donor concentration rises to unity. The naphthalene data in fig. 3 show that when the lattice is filled with donor molecules, the relative integrated trap emission is very close to unity. Therefore, if we wish to model naphthalene with a two-dimensional random system and the transfer rate of eq. (33), we must pick S large enough, so that $I(C_D, C_T)$ is unity for the donor concentration corresponding to a filled lattice. Fig. 4B shows that the resulting curve will rise more abruptly than the experimental points in fig. 3. The finite ranged transfer rate of eq. (33) results in a trapping onset much more sudden than that displayed by the singlet naphthalene data. We can conclude that the existence of a long-range tail in the transfer rate has a great effect on the observable $I(C_D, C_T)$.

Blumen and Silbey have formulated a kinetic model of transport and trapping of excitations in disordered systems [17], which fits the singlet and triplet naphthalene data obtained by Kopelman and co-workers [6–10], as well as data from a similar series of experiments performed by Colson and co-workers on benzene crystals, a three-dimensional system [15]. The benzene data show similar sharp rises in trapping efficiency at a critical donor concentration. Blumen and Silbey also found that a $1/r^{14}$ transfer rate gives the best fit to the naphthalene singlet data. Their expression for $I(\tilde{C})$ has a simple form:

$$I(\tilde{C}) = [1 + (\tilde{C})^{1-m/2}]^{-1}, \tag{34}$$

where m is the exponent in the multipolar transfer rate. The agreement between eq. (34) and our numerically calculated two-body $I(\tilde{C})$ is very good and improves with increasing $\tilde{C}$. For comparison, we have examined the mathematically convenient case of $m = 4$, for which $I(C_D, C_T)$ may be written in closed form. In the $C_T \to 0$ limit, $I(C_D, C_T)$ has a different form than that predicted by eq. (34), but goes over to eq. (34) in the $C_D \to \infty$ limit. For small C_T, the onset of trapping occurs at large C_D, so for the concentration range of interest, the two-body approximation to the master equation Green function and the kinetic model of Blumen and Silbey give numerically similar results for $I(\tilde{C})$. Both models predict that $I(\tilde{C})$ will have the same shape for a three-dimensional system with a $1/r^{21}$ transfer rate as for a two-dimensional system with a $1/r^{14}$ transfer rate. Because of the strongly anisotropic excitation transfer interactions in naphthalene, a two-dimensional isotropic model is a more sensible choice than a three-dimensional one. Also, as discussed in section 5, the $1/r^{14}$ rate corresponding to an octupole interaction is a physically reasonable one.

Despite the agreement between the kinetic model of Blumen and Silbey and the self-consistent Green function approach described here in the case of the steady-state observable $I(\tilde{C})$, the two models are by no means equivalent. The hopping model of Blumen and Silbey neglects back transfer processes, in which an excitation which is transferred away from an excited donor is eventually transferred back to the initially excited donor. The two-body Green function described here includes an infinite subset of the graphs representing such processes. Therefore, our model is expected to give more accurate results for time-dependent observables.

5. Conclusions

The agreement between the singlet naphthalene data and our model, as shown in fig. 3, indicates that as far as this observable is concerned, transport in disordered mixed molecular crystals is well described by the master equation, eq. (1). In our model, the singlet naphthalene data was best fit by a $1/r^{14}$ transfer rate, as it was in the work of Blumen and Silbey [17]. This transfer rate corresponds to an octupole–octupole interaction. This result is not surprising, since the transition dipole is known to be very small, ≈ 0.03 Å, and cannot account for the pure naphthalene crystal exciton band structure [18]. The octupole–octupole interaction is the next symmetry allowed term in a multipole expansion of the intermolecular interaction [18]. Craig and Walmsley have shown that the Davydov splitting in pure napthalene can be accounted for in terms of octupole–octupole interactions [18]. Hong and Kopelman [19] have also calculated octupole parameters for naphthalene from experimentally determined interaction energies between pairs of translationally equivalent sites in the crystal. However, these parameters do not agree quantitatively with the ones arrived at by Craig and Walmsley. Thus, the applicability of the octupole model to the naphthalene intermolecular interaction remains in question.

Our model indicates that the shape of the $I(C_D, C_T)$ curves is strongly dependent on the range of the intermolecular interaction. In particular, a dipole–dipole interaction results in a very different shape than that observed in the experiments on naphthalene and benzene. We therefore predict that if experiments analogous to those of Kopelman et al. [6–10] and Colson et al. [15] were carried out on a mixed crystal in which the molecular interactions could be described by dipole–dipole interactions, the typical sharp trapping onset would not be observed.

Acknowledgement

We would like to thank a referee for useful comments on this manuscript. This work was supported by the National Science Foundation, Division of Materials Research, grant DMR 79-20380. In addition, RFL thanks the National Science Foundation for a Predoctoral Fellowship.

References

[1] R.F. Loring, H.C. Andersen and M.D. Fayer, J. Chem. Phys. 76 (1982) 2015.
[2] C.R. Gochanour, H.C. Andersen and M.D. Fayer, J. Chem. Phys. 70 (1979) 4254.
[3] Th. Förster, Ann. Physik Leipzig 2 (1948) 55.
[4] R.M. Hochstrasser and J.D. Whiteman, J. Chem. Phys. 56 (1972) 5945;
D.M. Burland, J. Chem. Phys. 59 (1973) 4283;
D.M. Burland and R.M. Macfarlane, J. Luminescence 12 (1976) 213.
[5] A.H. Francis and C.B. Harris, Chem. Phys. Letters 9 (1971) 181;
D.D. Dlott and M.D. Fayer, Chem. Phys. Letters 41 (1976) 305;
D.D. Dlott, M.D. Fayer and R.D. Wieting, J. Chem. Phys. 69 (1978) 2752;
A.S. van Strien, J.F.C. van Kooten and J. Schmidt, Chem. Phys. Letters 76 (1980) 7.
[6] R. Kopelman, in: Topics in applied physics, Vol. 49, eds. W.M. Yen and P.M. Seltzer (Springer, Berlin, 1981) p. 241.
[7] R. Kopelman, E.M. Monberg, F.W. Ochs and P.N. Prasad, Phys. Rev. Letters 34 (1975) 1506.
[8] R. Kopelman, E.M. Monberg and F.W. Ochs, Chem. Phys. 21 (1977) 373.
[9] R. Kopelman, E.M. Monberg and F.W. Ochs, Chem. Phys. 19 (1977) 413.
[10] D.M. Hanson, J. Chem. Phys. 52 (1970) 3409.
[11] D.D. Smith, R.D. Mead and A.H. Zewail, Chem. Phys. Letters 50 (1977) 358.
[12] S.R. Broadbent and J.M. Hammersley, Proc. Cambridge Phil Soc. 53 (1957) 629.
[13] C.R. Gochanour and M.D. Fayer, J. Phys. Chem. 85 (1981) 1989.
[14] H. Stehfest, Commun. Ass. Comput. Mach. 13 (1970) 47, 624.
[15] S.D. Colson, R.E. Turner and V. Vaida, J. Chem. Phys. 66 (1977) 2187;
S.D. Colson, S.M. George, T. Keyes and V. Vaida, J. Chem. Phys. 67 (1977) 4941.
[16] T. Keyes and S. Pratt, Chem. Phys. Letters 65 (1979) 100.
[17] A. Blumen and R. Silbey, J. Chem. Phys. 70 (1979) 3707.
[18] D.P. Craig and S.H. Walmsley, Excitons in molecular crystals (Benjamin, New York, 1968) p. 107.
[19] H.-K. Hong and R. Kopelman, J. Chem. Phys. 55 (1972) 724.